

## *Transient Flow in Groundwater to Wells in Island Model Aquifer*

Makoto NISHIGAKI\* and Ichiro KONO\*

(Received October 31, 1979)

### Synopsis

In order to apply the numerical method to practical groundwater flow problem in the field, the hydraulic properties must be estimated. In this paper, new methods of analyzing drawdown tests were developed and illustrated with some examples to determine hydraulic properties of aquifer. Drawdown tests sometimes have to be performed near the boundary of the aquifer or in the much groundwater supplied aquifer. In such instances, the assumption that the aquifer is of infinite areal extent is no longer valid. Therefore the analytical solutions of unsteady flow due to drawdown test are derived in the conception of "Island Model" that the shape of groundwater level is fixed by the circular water supply which is equilibrium with the pumping rate. By using these solutions, new methods of analyzing drawdown tests which are performed in a confined aquifer and an unconfined aquifer were given respectively and the effect of influence region was evaluated. The example analysis to determine permeability and storage coefficient were shown. As the results, the propriety of the solutions is verified comparing the analytical results with the drawdown test data taken from a real aquifer project.

---

\* Department of Civil Engineering.

## 1. Introduction

In Theis' or Jacob's method, the assumption has been made that the horizontal extent of the aquifer was so great that for mathematical purposes it could be considered as an infinite radial system. However, adjusting drawdown test data gotten within relatively large time, the drawdowns in an observation well are often no longer dependent of time and their behaviors become nearly in steady state. It is difficult to explain this behavior by using Theis' assumption that water is supplied from an infinite radial region.

To give an explanation of this reason, it is considered that the drawdown within relatively large time becomes to keep the equilibrium with surrounding water supply, that is, the existence of an influence region of which radial distance keeps the balance against the pumping rate must be considered. Namely, the head around this region is equal to the initial head of groundwater.

This conception in which that model is named "Island Model" has been applied for the model of analysis in steady state drawdown test for a long time, but not the analysis of Island Model in unsteady state has been yet.

The Island Model is as same as the practical situation bounded in some manner, e.g., by a river or a reservoir. In this situation, the analysis of drawdown test has been solved by the method of images for boundary. This method, however, is confined to the assumption that the groundwater supply from many sources, that is, from river-bed water or neighboring groundwater is regarded as only one point well.

In this paper, first, the solutions of unsteady phreatic flow due to drawdown test are derived in the conception of "Island Model" that the shape of groundwater level is fixed by the circular water supply which is equilibrium with the pumping rate.

By using these solutions, the methods of analyzing drawdown test data in a confined aquifer and in an unconfined aquifer are given and the effect of influence region is evaluated. Furthermore, the analyses which have been separated in each cases of steady state and unsteady state pumping test are consolidated.

In this paper, the analysis stand on following assumptions.

- (1) Flow within the porous medium obeys Darcy's law.
- (2) The aquifer is homogeneous and isotropic with respect to permeability.
- (3) Storage coefficient is time independent.
- (4) Only single phase (or saturated) flow occurs in an aquifer.

- (5) The well is assumed to have no surface of seepage.
- (6) The pumping well used in the testing operations will also be assumed to be fully penetrating and to operate at a constant rate of withdrawal.

## 2. Analytical Solution for Island Model Drawdown Test in a Confined Aquifer

Indicating in introduction, the Theis' analytical solution heretofore in use was derived on the assumption that water is supplied from the region of infinite distance in drawdown test. Yielding this assumption, the radial distance ( $r$ ) from drawdown test well to the observation well and the time ( $t$ ) since pumping starts are always treated in the form of  $(t/r^2)$  or the inverse form of that, and drawdown test data performed in ideal conditions can be plotted on a curve independently of the position of wells.

But when drawdown data, which were obtained within large pumping time, are adjusted according to Theis' or Jacob's method, the results for each observation well are on the curve of Theis-Jacob's analytical solution until some time, and then they depart from that curve, that is, each curve of them becomes parallel to the abscissa independently of time.

To explain this reason, it is able to consider that there is a constant head boundary in finite radius ( $R$ ) as shown in Fig.2.1.

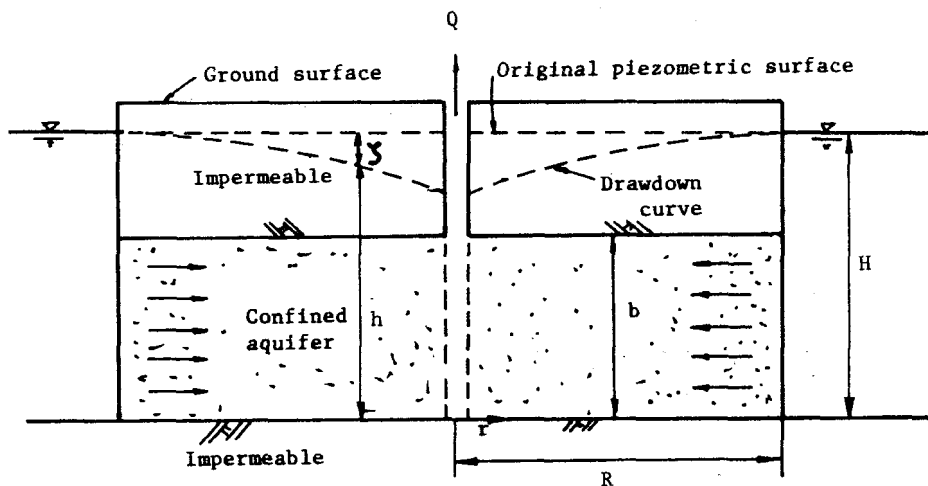


Fig.2.1 Nonsteady radial flow to a well penetrating a confined aquifer on an island

In this section, the solution of unsteady radial flow in a confined aquifer will first be derived, after which the method of analyzing drawdown test data will be given.

### 2.1 Basic equation and solution

The partial differential equation that describes the fluid movement in this system is again

$$\frac{\partial^2 \zeta}{\partial r^2} + \frac{1}{r} \frac{\partial \zeta}{\partial r} = \frac{1}{\alpha_s} \frac{\partial \zeta}{\partial t} \quad (2.1)$$

where  $\alpha_s$  is hydraulic diffusivity of aquifer ( $=K/S_s$ ) and  $\zeta$  is drawdown in aquifer ( $=H-h$ ).

Eq.(2.1) must be solved subject to following conditions,

$$\zeta(r, 0) = 0 \quad (\text{head initially constant}) \quad (2.2)$$

$$\zeta(R, t) = 0 \quad (\text{constant head at water boundary}) \quad (2.3)$$

$$\lim_{r \rightarrow 0} r \frac{\partial \zeta}{\partial r} = - \frac{Q}{2\pi K b} \quad (\text{flow rate into well of zero radius remains constant}) \quad (2.4)$$

To solve the initial boundary value problem given by Eqs.(2.2), (2.3), and (2.4), Laplace transformation is applied to Eq.(2.1) using initial condition Eq.(2.2)

$$\frac{\partial^2 \bar{\zeta}}{\partial r^2} + \frac{1}{r} \frac{\partial \bar{\zeta}}{\partial r} - q^2 \bar{\zeta} = 0 \quad (0 < r \leq R) \quad (2.5)$$

where  $q^2 = p/\alpha_s$ ,  $p$  is the parameter of Laplace transform and  $\bar{\zeta}$  is Laplace transform of  $\zeta$ .

The boundary conditions Eq.(2.3) and Eq.(2.4), treated in the same way, give

$$\bar{\zeta}(R, p) = 0 \quad (2.6)$$

$$\lim_{r \rightarrow 0} r \frac{\partial \bar{\zeta}}{\partial r} = - \frac{Q}{2\pi K b} \frac{1}{p} \quad (2.7)$$

The solution of Eq.(2.5) will be of the form

$$\bar{\zeta} = A I_0(qr) + B K_0(qr) \quad (2.8)$$

where  $I_0(qr)$  is the zeroth order modified Bessel function of the first kind and  $K_0(qr)$  is the zeroth order modified Bessel function of the second kind. Substituting Eq.(2.8) in Eqs.(2.6), (2.7) and solving for A and B,  $\bar{\zeta}$  is gotten finally.

$$\bar{\zeta} = \frac{Q}{2\pi Kb} \{ \bar{g}_1 - \bar{g}_2 \cdot \bar{g}_3 \} \quad (2.9)$$

where

$$\bar{g}_1 = K_0(qr)/p \quad (2.10)$$

$$\bar{g}_2 = K_0(qR) \quad (2.11)$$

$$\bar{g}_3 = I_0(qr)/pI_0(qR) \quad (2.12)$$

Eqs.(2.10),(2.11), and (2.12) are now respectively, determined by the Inversion Theorem.

$$g_1 = \frac{1}{2} \int_{r^2/4\alpha_s t}^{\infty} \frac{e^{-u}}{u} du \quad (2.13a)$$

$$g_2 = \frac{1}{2t} \exp(-R^2/4\alpha_s t) \quad (2.13b)$$

$$g_3 = 1 - \frac{2}{R} \sum_{n=1}^{\infty} \exp(-\alpha_s \alpha_n^2 t) \times J_0(r\alpha_n) / \alpha_n^3 J_1(R\alpha_n) \quad (2.13c)$$

where  $\alpha_n$  are the roots of the characteristic equation

$$J_0(r\alpha_n) = 0 \quad (2.14)$$

By using the Duhamel Formulas and combining these results the solution of  $\bar{\zeta}$  is derived,

$$\begin{aligned} \zeta = & \frac{Q}{4\pi Kb} \left[ \int_{r^2/4\alpha_s t}^{\infty} \frac{e^{-\lambda}}{\lambda} d\lambda - \int_{R^2/4\alpha_s t}^{\infty} \frac{e^{-\lambda}}{\lambda} d\lambda \right] \\ & + \frac{Q}{2\pi KbR} \int_0^t \frac{1}{\tau} \exp[-R^2/4\alpha_s \tau] \sum_{n=1}^{\infty} \exp[-\alpha_s \alpha_n^2 (t-\tau)] \\ & \times \frac{J_0(r\alpha_n)}{\alpha_n^3 J_1(r\alpha_n)} d\tau \end{aligned} \quad (2.15)$$

If R becomes an infinite radial distance in Eq.(2.15), the result is the same of Theis' solution.

In general the value of permeability ( $K$ ) is  $K=1 \times 10^{-2} \sim 10^{-3}$  (cm/sec) and the value of specific storage ( $S_s$ ) is  $S_s=1 \times 10^{-5} \sim 10^{-6}$  (cm<sup>-1</sup>), then the value of the ratio ( $\alpha_s=K/S_s$ ) becomes about  $\alpha_s=10^2 \sim 10^4$  (cm<sup>2</sup>/sec). Therefore, on the right hand side of Eq.(2.15), the third term is as small as negligible comparing with the first and second terms, and so the approximate solution of drawdown ( $\zeta$ ) is given by

$$\begin{aligned} \zeta & \doteq \frac{Q}{4\pi Kb} \left[ \int_{r^2/4\alpha_s t}^{\infty} \frac{e^{-u}}{u} du - \int_{R^2/4\alpha_s t}^{\infty} \frac{e^{-u}}{u} du \right] \\ & = -\frac{Q}{4\pi Kb} [ E_1(-r^2/4\alpha_s t) - E_1(-R^2/4\alpha_s t) ] \\ & = \frac{Q}{4\pi Kb} [ W(r^2/4\alpha_s t) - W(R^2/4\alpha_s t) ] \end{aligned} \quad (2.16)$$

where  $E_1(x)$  is the exponential integral and  $W(x)$  is the well function. It can be expanded as a convergent series so that  $W(x)$  becomes

$$W(x) = -0.5772 - \ln(x) + x - \frac{x^2}{2 \cdot 2!} + \frac{x^3}{3 \cdot 3!} \dots \dots \dots \quad (2.17)$$

For large values of time ( $t$ ),  $x$  is small, so that the series terms in in Eq.(2.17) become negligible after the first two terms. As a result, the drawdown can be expressed by the asymptote

$$\begin{aligned} \zeta & \doteq \frac{2.30Q}{4\pi Kb} [ (\log_{10}(t/r^2) - \log_{10}(S_s/2.25K) \\ & \quad - (\log_{10}(t/R^2) - \log_{10}(S_s/2.25K)) ] \\ & = \frac{2.30Q}{2\pi Kb} \log_{10}(R/r) \end{aligned} \quad (2.18)$$

Eq.(2.18) is the solution of the model shown in Fig.2.1 for steady state flow.

## 2.2 Effects of constant head at outer boundary

Eq.(2.16) is used to evaluate  $\zeta^*$  as a function of  $t^*$  for values of  $R^*$  ranging from 1.5 to 100, in which

$$\zeta^* = 4\pi Kb\zeta/Q \quad (2.19)$$

$$t^* = (K/S_s)(t/r^2) \quad (2.20)$$

$$R^* = R/r \quad (2.21)$$

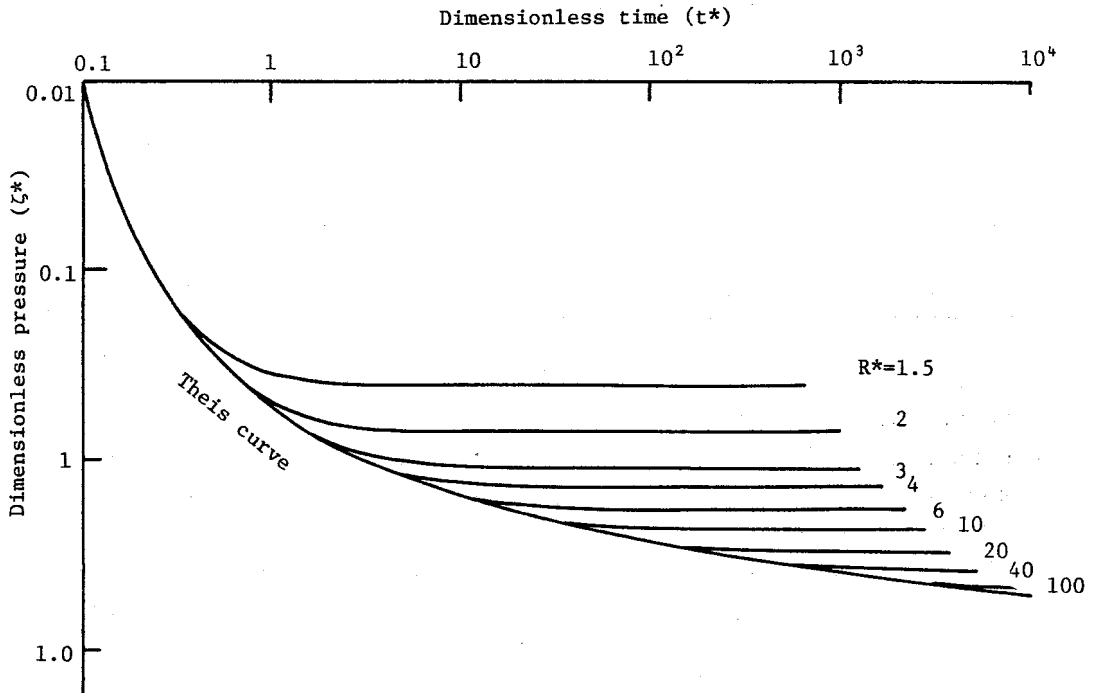


Fig.2.2  $\zeta^*$  versus  $t^*$  for limited aquifer with constant head boundary

Fig.2.2 shows the resulting family of curves for several values of  $R^*$ . The type curves depart from the Theis curve in pairs with the point of departure depending on the value of  $R^*$ , and it is distinct that the drawdown in the aquifer bounded by constant head becomes steady state earlier than that in the infinite extent aquifer. From Fig.2.2 it is also obvious that if the value of  $R^*$  is larger than 100, the effects of the influence region is negligible. In other words, the drawdown in such a condition is not affected by constant head boundary. An interesting way of looking at this result has been suggested by Mononobe for steady well problem. To use his own words [1]: "In actual problem, the influence region extends since pumping starts, whereas, by reason of the extent of aquifer, the effects of other wells, and the infiltration of rain, the head at circular boundary does not have to be constant. Therefore the influence region is not always expanding into the infinite region."

If a large pumping rate is continued the groundwater around well may be dried up. In general, it would be safe to calculate the drainage rate assuming the influence region must be within the range from 500 meters to 1000 meters. " We perform the pumping test at the condition that the observation wells are set within about 20 meters of the radial distance from pumping well. And so the value of  $R^* > 100$  means that the influence region must be within 2000 meters. This is a theoretical explanation of the assumption based on experiences.

### 2.3 Method of analyzing field data

The engineer wishes to determine the values of the aquifer constants ( $K, S_g$ ) and the radial distances of the influence region, ( $R$ ). The properties of the aquifer will presumably be known from earlier drawdown tests, and the approximate radial distances of the influence region will have been predicted by geological reconnaissance.

In this section, the differences that appear in the data, and the adaptations that must be made to the methods of interpretation, due to the presence of boundary will be given.

#### Log-Log Method

The presence of a suspected circular boundary within the region of influence of the drawdown test may be indicated by the inability to match the log-log field data plot on time versus drawdown with the Theis' method. Eq.(2.16) is rewritten by using dimensionless drawdown ( $\zeta^*$ ) and time ( $t^*$ )

$$\zeta^* = -E_1(-r^2/t^*) + E_1(-R^2/t^*) \quad (2.22)$$

where

$$\left. \begin{aligned} \zeta^* &= 4\pi K b \zeta / Q \\ t^* &= 4\alpha_s t \end{aligned} \right\} \quad (2.23)$$

It is necessary to assume the value of  $R$  for calculating Eq.(2.22) in numerical method. As indicating in introduction, the value of  $R$  is defined by the conditions of the pumping rate and that of hydrology.

If a drawdown test is run for a relatively long time, the drawdown will become in steady state. In this state the drawdown is given by Eq.(2.18), the value of  $R$  can be calculated as follows:



$$R = r \cdot \exp(2\pi K b \zeta / Q) \quad (2.24)$$

In Eq.(2.24), the values of  $r$ ,  $\zeta$ ,  $b$ , and  $Q$  are from the relatively long time drawdown test. The permeability ( $K$ ) is obtained from the application of Jacob's method. With this method, an observation well near the pumping well is needed. Such a well will have a high value of  $R^*(=R/r)$ , and as reference to Fig.2.1 shows, deviation from the Theis curve due to the effect of the boundary will not occur until considerable pumping time has elapsed. A rough estimate of permeability ( $K$ ) can be calculated on the basis of the early drawdown data from such a well. A rough calculation of the value of  $R$  is gotten. Knowing the values of  $R$ , one can prepare a graph of  $\log \zeta^*$  versus  $\log t^*/r^2$  depending on the value of  $r$  from Eq.(2.22). When the drawdown data from each observation well has been plotted log-log paper with the same dimensions per cycle as used above, one matches the field results to the theoretical curve.

When the curves are matched, one can read the dimensionless parameters that correspond to each point of field data. An equivalent value  $\zeta^*$  can be determined for any  $\zeta$  measured in the observation well and an equivalent value of  $t^*/r^2$ , for the corresponding value of real time,  $t/r^2$ . The permeability can be calculated from Eq.(2.23).

$$K = \frac{Q \zeta^*}{4\pi b \zeta} \quad (2.25)$$

and the compressibility factor can be calculated from Eq.(2.23)

$$s_s = 4K(t/r^2)/(t^*/r^2) \quad (2.26)$$

Moreover by the data of drawdown for a relatively large time, the permeability can be obtained from Eq.(2.18) in the another method.

$$K = \frac{2.30Q}{2\pi b \zeta} \log_{10}(R/r) \quad (2.27)$$

#### 2.4 Analysis of drawdown test data

The following discussion gives example calculations of the method given above. The drawdown test data are taken from a real aquifer project that is located near Lake Shinji, Shimane Pref. in Japan.

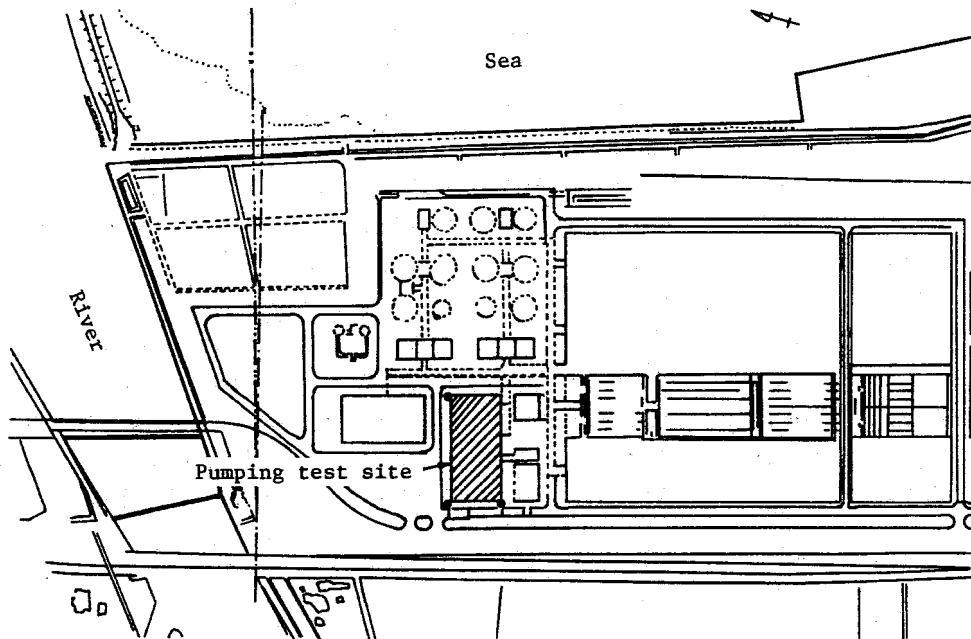


Fig.2.3 Plane view of the drawdown test site

The plane view of this region is shown in Fig.2.3. This region is bounded by the river on the west and by sea on the north. The geological condition obtained from well logs is shown in Fig.2.4. Two sand-gravel layers revealed as confined aquifers exist in this region.

Firstly the drawdown test performed in the lower part confined aquifer is going to be analyzed for example using an average rate of  $Q=4.17 \times 10^3 \text{ cm}^3/\text{sec}$ . The thickness of this aquifer is revealed  $b=5.2\text{m}$ . The drawdown test data is analyzed by Jacob's method as shown in Fig. 2.5, a rough estimate of permeability is obtained  $K=5.78 \times 10^{-2} \text{ cm/sec}$ .

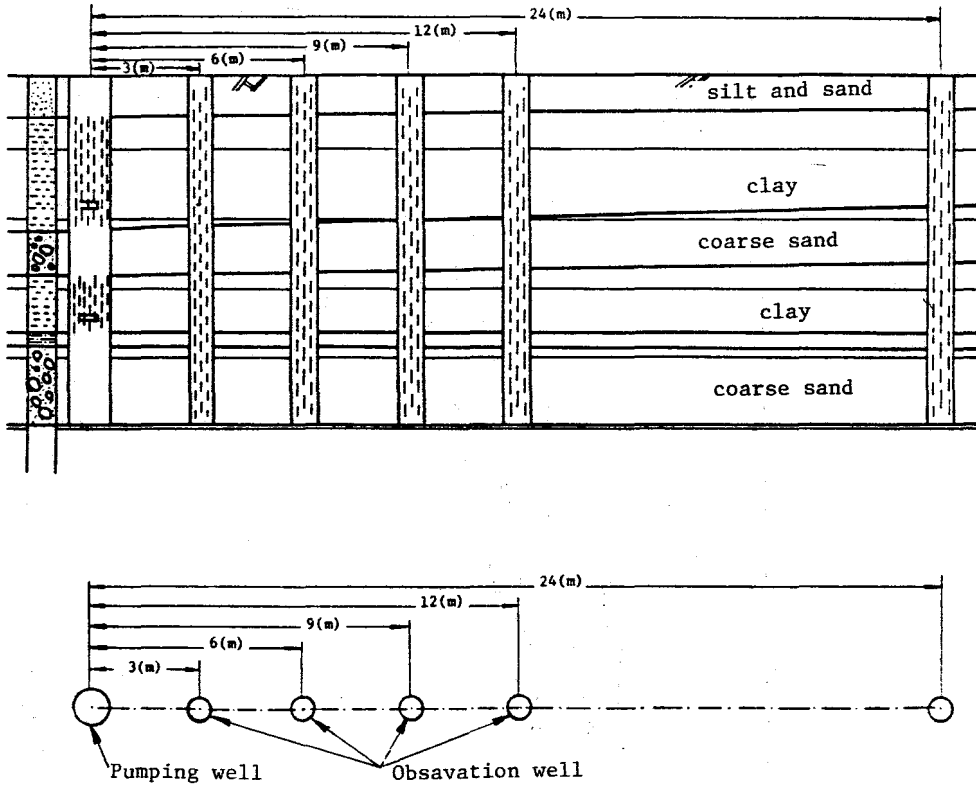


Fig.2.4 Hydrogeological cross-section through the experimental group of wells

For the relatively large time (4 hours) drawdown test data of the observation well ( $r=12\text{m}$ ), the drawdown which is regarded as steady state is  $\zeta=52\text{cm}$ . Interpolating these parameters in Eq.(2.24). The rough calculation of the value of  $R$  is gotten

$$R = r \cdot \exp(2\pi kb\zeta/Q) \doteq 126\text{m}$$

The radial distance from pumping well to the river and sea is about 175m. From these results the value of  $R$  is estimated the four cases, that is, 100m, 125m, 150m, and 175m. Matching the field results to the theoretical curves for each value of  $R$ , the field data make a satisfactory fit to the theoretical curves for  $R=150\text{m}$  as shown in Fig.2.6.

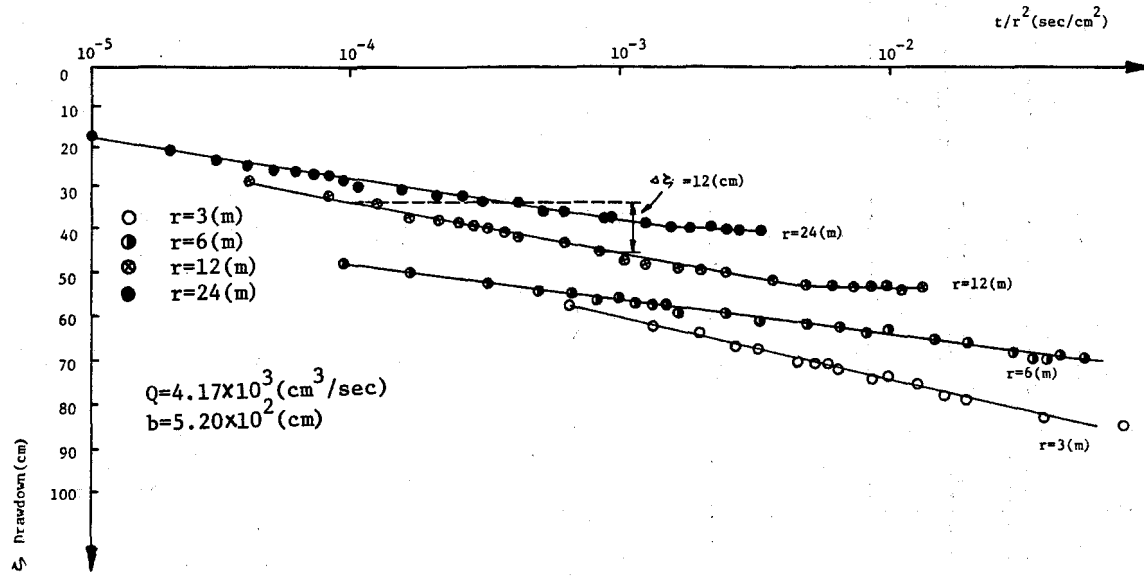


Fig.2.5 Method of Jacob's analysis ( $z-t/r^2$ )

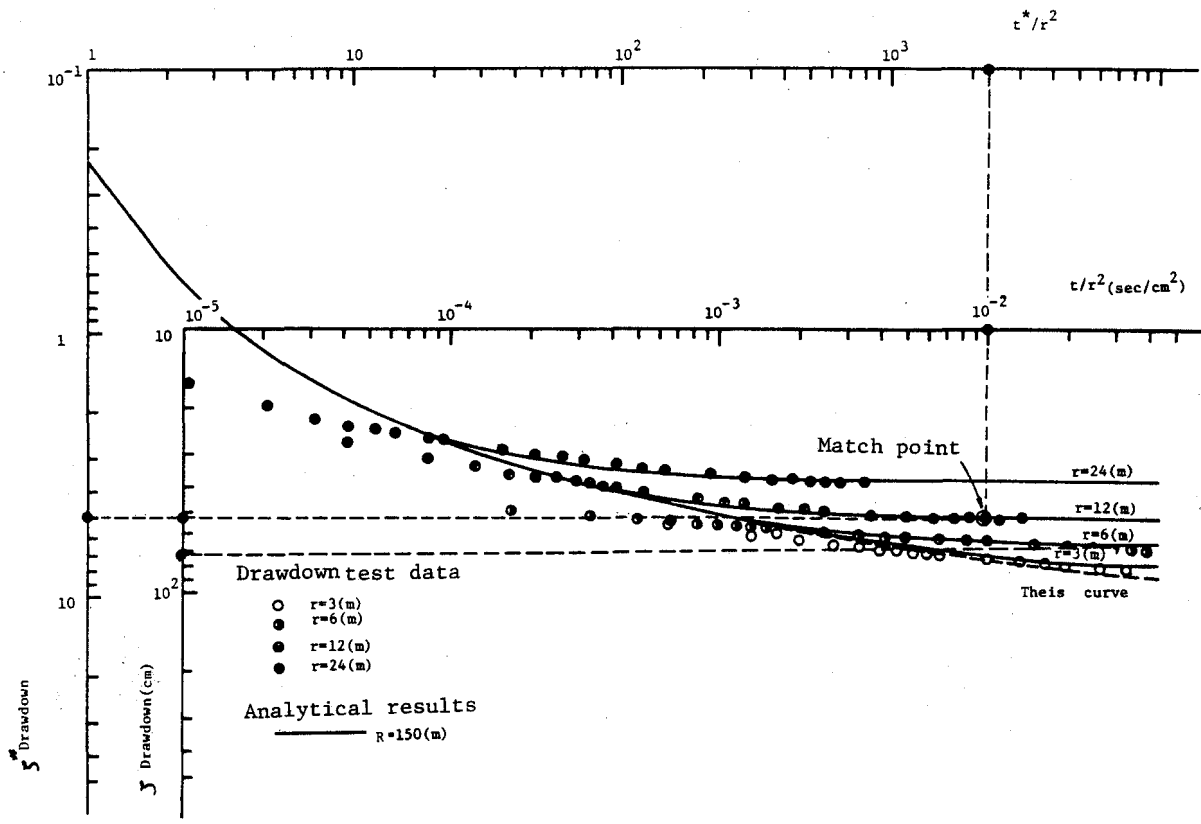


Fig.2.6 Method of superposition for finite region solution

At the match point where  $\zeta^*=5.0$ , and  $t^*/r^2=2.3 \times 10^3$ , one reads  $\zeta=5.2 \times 10 \text{ cm}$  and  $t/r^2=10^{-2} \text{ sec/cm}^2$  for  $r=12 \text{ m}$ .

From Eq.(2.25), the permeability can be calculated

$$K = \frac{5.0 \times 4.17 \times 10^3}{4 \times \pi \times 520 \times 5.2 \times 10} = 6.14 \times 10^{-2} \text{ (cm/sec)}$$

From Eq.(2.26), the compressibility factor can be calculated

$$S_s = \frac{4 \times 6.14 \times 10^{-2} \times 10^{-2}}{2.30 \times 10^3} = 1.07 \times 10^{-6} \text{ cm}^{-1}$$

Interpolating these calculated values in Eq.(2.16), the result of comparison of theoretical curves with drawdown test data is shown in Fig.2.7. It is definite that theoretical curves give a good match with the drawdown test data. From the steady state data, the permeability can be calculated from Eq.(2.27) interpolating  $R=150 \text{ m}$ ,  $r=12 \text{ m}$ ,  $\zeta=52 \text{ cm}$ ,  $Q=4.17 \times 10^3 \text{ cm}^3/\text{sec}$ ,  $b=5.2 \text{ m}$

$$K = \frac{2.30 \times 4.17 \times 10^3}{2 \times \pi \times 520 \times 5.2} \log_{10}(150/12) = 6.20 \times 10^{-2} \text{ (cm/sec)}$$

Secondly the drawdown test performed in the upper part confined aquifer is going to be analyzed for the second example using an average rate of  $Q=3.69 \times 10^2 \text{ cm}^3/\text{sec}$ . The thickness of this aquifer is revealed  $b=2.10 \text{ m}$ . With the same way of the first example,  $R$  is estimated  $R=13.5 \text{ m}$ . At the match point where  $\zeta^*=2.2 \times 10^{-1}$  and  $t^*/r^2=13$ , one reads  $\zeta=4.0 \text{ cm}$ ,  $t/r^2=10^{-2} \text{ sec/cm}^2$  as shown in Fig.2.8. From Eqs.(2.25), (2.26) the permeability and the compressibility factor

$$K = \frac{369 \times 2.2 \times 10^{-1}}{4 \times \pi \times 210 \times 4.0} = 7.69 \times 10^{-3} \text{ (cm/sec)}$$

$$S_s = \frac{4 \times 7.69 \times 10^{-3} \times 10^{-2}}{13} = 2.37 \times 10^{-5} \text{ (cm}^{-1}\text{)}$$

Interpolating these values into Eq.(2.16), the result of comparison of theoretical curves with the drawdown test data is shown in Fig.2.9. In this case theoretical curves also give a good match with the drawdown test data.

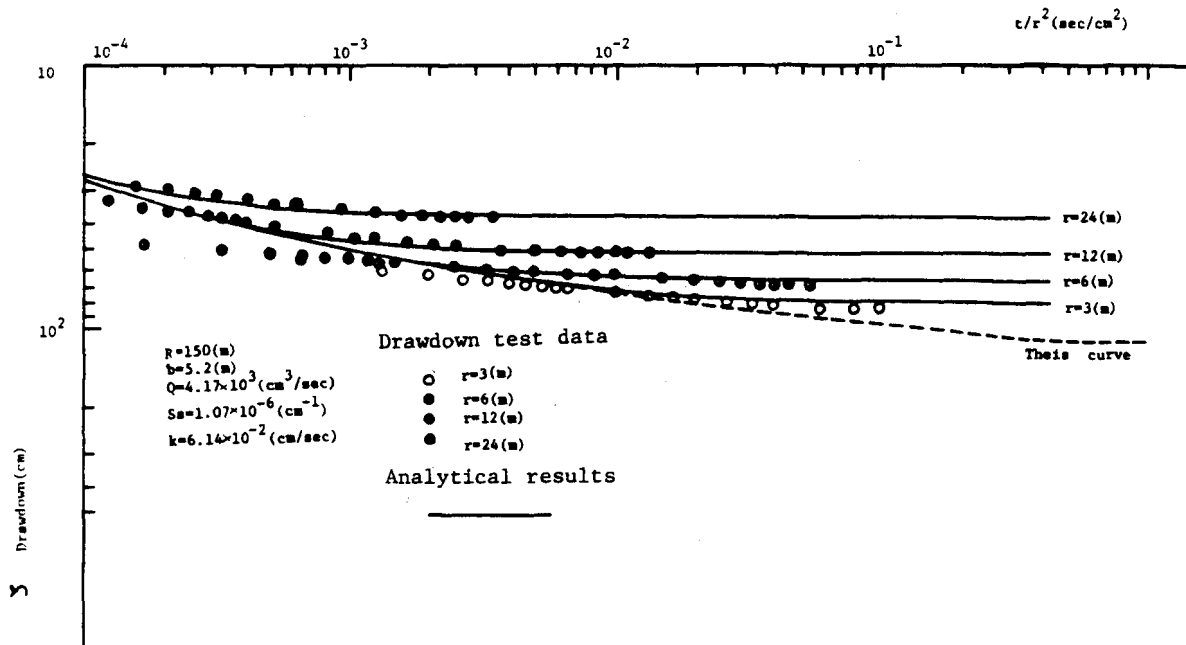


Fig.2.7 Comparison of the analytical results and drawdown test data

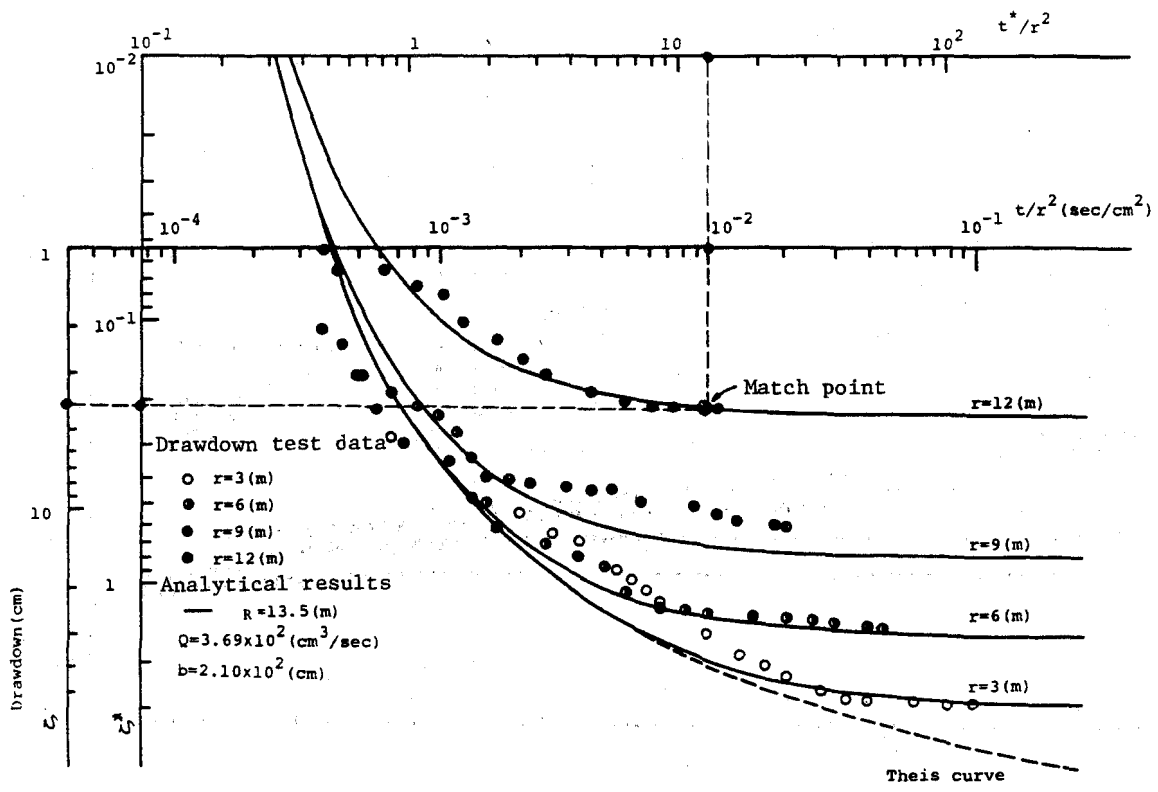


Fig.2.8 Method of superposition for finite region solution



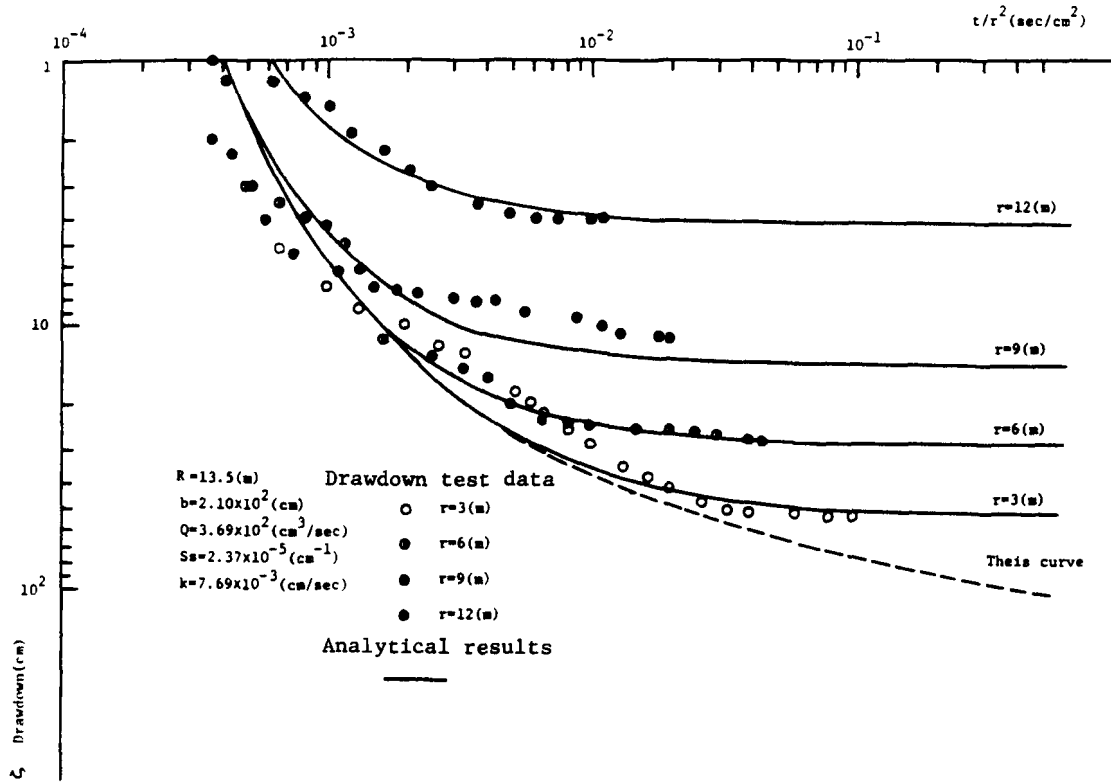


Fig.2.9 Comparison of the analytical results and drawdown test data

### 3. Analytical Solution for Island Model Drawdown Test in an Unconfined Aquifer

In section 2, the analytical solution on a confined aquifer has been derived and example calculations are given.

In this section, consider an unconfined aquifer of finite lateral extent that rests on an impermeable horizontal layer such as that shown schematically in Fig.3.1. A well completely penetrating the aquifer discharges at a constant rate  $Q$ , and water is released from storage by gravity drainage at the free surface, neglecting the storage by compaction of the aquifer material expansion of the water.

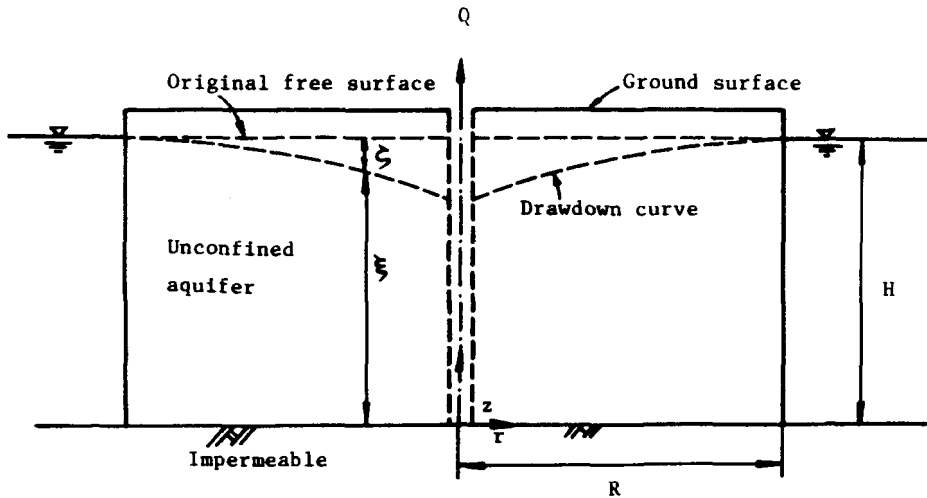


Fig.3.1 Nonsteady radial flow to a well penetrating an unconfined aquifer on an island

#### 3.1 Basic equation and solution

With the assumptions which are described in introduction, the governing partial differential equation are given

$$\frac{\partial^2 \zeta}{\partial r^2} + \frac{1}{r} \frac{\partial \zeta}{\partial r} + \frac{\partial^2 \zeta}{\partial z^2} = 0 \quad (0 < z < \xi, 0 < r < R) \quad (3.1)$$

Eq.(3.1) must be solved subject to following conditions

$$\left. \begin{aligned} \zeta(r,z,0) &= 0 \\ \xi(r,0) &= H \end{aligned} \right\} \text{ (head initially constant)} \quad (3.2)$$

$$\zeta(R,z,t) = 0 \quad \text{(constant head at out boundary)} \quad (3.3)$$

$$\frac{\partial \zeta}{\partial z}(r,0,t) = 0 \quad \text{(on no flow across lower boundary)} \quad (3.4)$$

$$\lim_{r \rightarrow 0} \int_0^{\xi} r \frac{\partial \zeta}{\partial r} dz = -\frac{Q}{2\pi K} \quad \text{(at the well-bore)} \quad (3.5)$$

$$\left. \begin{aligned} \frac{\partial \zeta}{\partial r} n_r + \frac{\partial \zeta}{\partial z} n_z &= \frac{S_y}{K} \frac{\partial \zeta}{\partial t} n_z \\ \xi(r,t) &= H - \zeta(r,\xi,t) \end{aligned} \right\} \text{ (on free-surface boundary)} \quad (3.6)$$

where  $n_r$ ,  $n_z$  is the component of unit outer normal vector in  $r$  direction and in  $z$  direction respectively.  $S_y$  is the effective porosity or specific yield.

Eqs.(3.1) - (3.6) can be linearized by using a perturbation technique similar to that described by Dagan [2,3], provided the aquifer is thick enough and  $\zeta$  remains much smaller than  $\xi$ . Here this technique leads to a first order linearized approximation, obtained simply by shifting the boundary condition from the free surface to the horizontal plane  $z=H$ .

This eliminates  $\xi$  from Eqs.(3.2) - (3.6), one obtains

$$\frac{\partial^2 \zeta}{\partial r^2} + \frac{1}{r} \frac{\partial \zeta}{\partial r} + \frac{\partial^2 \zeta}{\partial z^2} = 0 \quad (3.7)$$

$$\zeta(r,z,0) = 0 \quad (3.8)$$

$$\zeta(R,z,t) = 0 \quad (3.9)$$

$$\frac{\partial \zeta}{\partial z}(r,0,t) = 0 \quad (3.10)$$

$$\lim_{r \rightarrow 0} r \frac{\partial \zeta}{\partial r} = -\frac{Q}{2\pi KH} \quad (3.11)$$

$$\frac{\partial \zeta}{\partial z}(r,H,t) = -\frac{1}{\alpha_y} \frac{\partial \zeta}{\partial t}(r,H,t) \quad (3.12)$$

where  $\alpha_y = K/S_y$  (3.13)

In solving the initial boundary value problem posed by (3.8) - (3.12), it is convenient to divide  $\zeta$  into two components

$$\zeta = \zeta_1(r, t) + \zeta_2(r, z, t) \quad (3.14)$$

Although both  $\zeta_1$  and  $\zeta_2$  satisfy Eqs.(3.7) - (3.10), there is a change in boundary conditions Eqs.(3.11) and (3.12), which now take the form

$$\frac{\partial^2 \zeta_1}{\partial r^2} + \frac{1}{r} \frac{\partial \zeta_1}{\partial r} = 0 \quad (3.15)$$

$$\zeta_1(R, 0) = 0 \quad (3.16)$$

$$\zeta_1(R, t) = 0 \quad (3.17)$$

$$\lim_{r \rightarrow 0} r \frac{\partial \zeta_1}{\partial r} = \frac{-Q}{2\pi KH} \quad (3.18)$$

$$\frac{\partial^2 \zeta_2}{\partial r^2} + \frac{1}{r} \frac{\partial \zeta_2}{\partial r} + \frac{\partial^2 \zeta_2}{\partial z^2} = 0 \quad (3.19)$$

$$\zeta_2(R, z, 0) = 0 \quad (3.20)$$

$$\zeta_2(R, z, t) = 0 \quad (3.21)$$

$$\frac{\partial \zeta_2}{\partial z}(r, 0, t) = 0 \quad (3.22)$$

$$\lim_{r \rightarrow 0} r \frac{\partial \zeta_2}{\partial r} = 0 \quad (3.23)$$

$$\frac{\partial \zeta_2}{\partial z}(r, H, t) = -\frac{1}{\alpha_y} \frac{\partial (\zeta_1 + \zeta_2)}{\partial t}(r, H, t) \quad (3.24)$$

When Laplace transform is applied to Eqs.(3.15) - (3.24) with respect to  $\zeta_1$  and  $\zeta_2$ , Eqs.(3.15) - (3.24) are given as follows;

$$\frac{\partial^2 \bar{\zeta}_1}{\partial r^2} + \frac{1}{r} \frac{\partial \bar{\zeta}_1}{\partial r} = 0 \quad (3.25)$$

$$\bar{\zeta}_1(R, p) = 0 \quad (3.26)$$

$$\lim_{r \rightarrow 0} r \frac{\partial \bar{\zeta}_1}{\partial r} = \frac{1}{p} \frac{-Q}{2\pi K H} \quad (3.27)$$

$$\frac{\partial^2 \bar{\zeta}_2}{\partial r^2} + \frac{1}{r} \frac{\partial \bar{\zeta}_2}{\partial r} + \frac{\partial^2 \bar{\zeta}_2}{\partial z^2} = 0 \quad (3.28)$$

$$\bar{\zeta}_2(R, H, p) = 0 \quad (3.29)$$

$$\frac{\partial \bar{\zeta}_2}{\partial z}(r, 0, p) = 0 \quad (3.30)$$

$$\lim_{r \rightarrow 0} r \frac{\partial \bar{\zeta}_2}{\partial r} = 0 \quad (3.31)$$

$$\frac{\partial \bar{\zeta}_2}{\partial z}(r, H, p) = -\frac{1}{\alpha_y} (\bar{\zeta}_1 + \bar{\zeta}_2) p \quad (3.32)$$

The solution of Eq.(3.25) with respect to  $\bar{\zeta}_1$  can be obtained with the conditions, Eqs.(3.26), (3.27).

$$\bar{\zeta}_1 = -\frac{Q}{2\pi K b} \frac{1}{p} \ln(r/R) \quad (3.33)$$

The solution of Eq.(3.28) with respect to  $\bar{\zeta}_2$  will be of the form

$$\bar{\zeta}_2 = A e^{\alpha z} J_0(\alpha r) + B e^{-\alpha z} J_0(\alpha r) \quad (3.34)$$

where  $J_0(x)$  is the Bessel function of order zero of the first kind. From the condition (3.30), Eq.(3.34) becomes

$$\bar{\zeta}_2 = A \cosh(\alpha z) J_0(\alpha r) \quad (3.35)$$

To satisfy the boundary condition Eq.(3.29)  $\alpha$  must be an infinite number of real positive roots

$$J_0(\alpha_n R) = 0 \quad (3.36)$$

$\alpha_n R$  is defined as  $\lambda_n$ , then Eq.(3.35) can be rewritten as

$$\bar{\zeta}_2 = \sum_{n=1}^{\infty} A_n \cosh(\lambda_n z/R) J_0(\lambda_n r/R) \quad (3.37)$$

The constant value  $A_n$  can be obtained from the condition Eq.(3.32),

$$\begin{aligned} & \sum_{n=1}^{\infty} A_n (\lambda_n/R) \sinh(\lambda_n H/R) J_0(\lambda_n r/R) \\ &= -(p/\alpha_y) [(Q_0/p) \ln(r/R) + \sum_{n=1}^{\infty} A_n \cosh(\lambda_n H/R) J_0(\lambda_n r/R)] \end{aligned} \quad (3.38)$$

and the expression above can be rewritten as

$$\sum_{n=1}^{\infty} A_n C_n J_0(\lambda_n r/R) = \ln(r/R) \quad (3.39)$$

where now

$$C_n = -(\alpha_y/Q_0) [ (\lambda_n/R) \sinh(\lambda_n H/R) + (p/\alpha_y) \cosh(\lambda_n H/R) ] \quad (3.40)$$

and

$$Q_0 = -Q/(2\pi kH) \quad (3.41)$$

On a given interval  $0 < r < R$  the right-hand side of Eq.(3.39) is expanded in the form of Fourier-Bessel series,

$$\ln(r/R) = \sum_{n=1}^{\infty} a_n J_0(\lambda_n r/R) \quad (3.42)$$

the Fourier constants  $a_n$  of  $\ln \frac{r}{R}$  in Eq.(3.42) are

$$a_n = \frac{2}{R^2 J_1^2(\lambda_n)} \int_0^R r [\ln(r/R)] J_0(\lambda_n r/R) dr \quad (3.43)$$

Integrating over  $r$  from 0 to  $R$ , one finds

$$a_n = -2/(\lambda_n^2 J_1^2(\lambda_n)) \quad (3.44)$$

From Eqs.(3.39), (3.42) and (3.44), the constants  $A_n$  are

$$A_n = a_n / C_n \quad (3.45)$$

Interpolating Eq.(3.45) into (3.38) and using (3.33), adding the transforms of both components gives

$$\bar{\zeta} = \bar{\zeta}_1 + \bar{\zeta}_2 = (Q_0/p) \ln(r/R) + \sum_{n=1}^{\infty} (a_n / C_n) \times \cosh(\lambda_n z/R) J_0(\lambda_n r/R) \quad (3.46)$$

The inversion of the Laplace transform of  $\bar{\zeta}$  is accomplished, one obtains the first order approximation to the original initial boundary value problem.

The final solution is expressed as follows;

$$\zeta = - \frac{Q}{2\pi KH} [ \ln(r/R) + \sum_{n=1}^{\infty} \frac{2J_0(\lambda_n r/R) \cosh(\lambda_n z/R) \exp[-t(\lambda_n K/RS_y) \tanh(\lambda_n H/R)]}{\lambda_n^2 J_1^2(\lambda_n) \cosh(\lambda_n H/R)} ] \quad (3.47)$$

In Eq.(3.47), let  $t$  become infinite the result becomes

$$\zeta = - \frac{Q}{2\pi KH} \ln(r/R) \quad (3.48)$$

this is just the steady state solution of the model shown in Fig.3.1.

### 3.2 Effects of constant head at outer boundary

To illustrate the analytical results, a computer program that permits to determine the dimensionless ratio  $\zeta^*$  ( $=2\pi KH\zeta/Q$ ) as a function of the dimensionless time  $t^*$  ( $=Kt/RS_y$ ) for given dimensionless values of  $r^*$  ( $=r/R$ ),  $z^*$  ( $=z/R$ ) and  $H^*$  ( $=H/R$ ), according to follow expression of Eq.(3.47) has been prepared.

$$\zeta^* = -\ln(r^*) - \sum_{n=1}^{\infty} \frac{2J_0(\lambda_n r^*) \cosh(\lambda_n z^*) \exp[-\lambda_n t^* \tanh(\lambda_n H^*)]}{\lambda_n^2 J_1^2(\lambda_n) \cosh(\lambda_n H^*)} \quad (3.49)$$

The program has been run for various combinations of the parameters. In Fig.3.2, drawdown curves at ( $z^*=1$ ) observation wells ( $r/R=100,20,10,5,4$ , and 2) are presented for  $R/H=10$ . The abscissa  $t^*/(r^*)^2$  ( $=\frac{RKt}{S_y r^2}$ ) is the independent variable in the Theis formula, whose drawdown curve has also been represented in Fig.3.2.

The type curves depart from the Theis curve in pairs with the point of departure depending on the value of  $R^*$  ( $=\frac{R}{r}$ ). It is noted on Fig.3.2, as same as the confined condition, that the drawdown in the aquifer bounded by constant head becomes steady state earlier than the drawdown in the infinite extent aquifer.

### 3.3 Method of analyzing field data

In an unconfined aquifer, the engineer wishes to determine the value of the aquifer constants ( $K, S_y$ ) and the radial distances of the influence region ( $R$ ) in the same way of the case in the confined aquifer. The geological condition of the aquifer is known from the well logs. Here, an analysis of the drawdown data in the observation wells is shown.

#### Log-Log Method

To prepare a graph of drawdown  $\log \zeta^*$  versus  $\log t^*$  for the appropriate  $r^*$  ( $=r/R$ ) between pumping well and observation wells from Eq.(3.49), it is necessary to obtain the values of  $R, H$ . The thickness



(H) of the aquifer can be obtained from the well logs and the measuring the existent ground water level. The value of R is assumed from the same way of confined aquifer, namely, if a drawdown test is run for relatively long time, the drawdown will become in steady state, and in this state the drawdown is given by Eq.(3.48). From that equation, the value of R can be calculated

$$R = r \cdot \exp(2\pi KH\zeta/Q) \quad (3.50)$$

In Eq.(3.50), though the known values are H,  $\zeta$ , and Q, the permeability (K) is unknown value. The permeability (K) is obtained from the application of Jacob's method. With this method, an observation well near the pumping well is needed. Such a well will have a high value of  $R^*(=R/r)$ , and as reference to Fig.3.2, deviation from the Theis curve due to the effect of the boundary will not occur until considerable pumping time has elapsed. A rough estimate of permeability (K) can be calculated on this basis of the early drawdown data from such a well. Interpolating these parameters into Eq.(3.50), a rough calculation of the value of R can be gotten. Getting the values of R, one can prepare a graph of  $\log\zeta^*$  versus  $\log t^*/r^2$  depending on the value of r from Eq.(3.49), in that equation

$$\zeta^* = 2\pi KH\zeta/Q \quad (3.51)$$

$$t^* = (K/S_y) \cdot t \quad (3.52)$$

By using the match point method, one can read the dimensionless parameters that correspond to each point of field data.

An equivalent value  $\zeta^*$  can be determined for any  $\zeta$  measured in the observation well and an equivalent value of  $t^*/r^2$ , for the corresponding value of real time,  $t/r^2$ . The permeability can be calculated from Eq.(3.51)

$$K = (Q/2\pi H)(\zeta^*/\zeta) \quad (3.53)$$

and the effective porosity can be calculated from Eq.(3.52)

$$S_y = K(t/t^*) \quad (3.54)$$

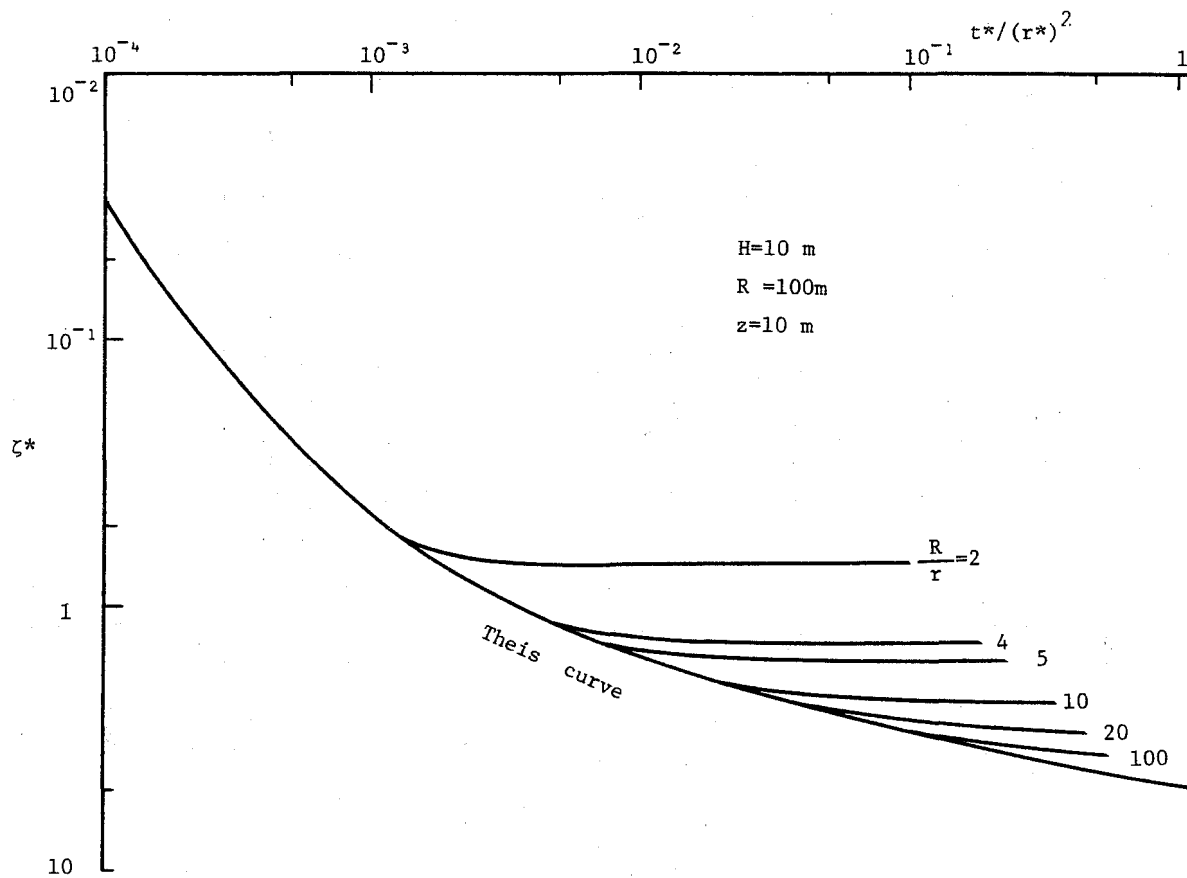


Fig.3.2 Analytical results for radii of flow region

### 3.4 Analysis of drawdown test data

The drawdown test data are taken from a real aquifer project that is located near Goshyo, Kyoto City in Japan. The geological condition obtained from well logs is shown in Fig.3.3. The drawdown test performed in the unconfined aquifer is going to be analyzed for example using an average rate of  $Q=2.67 \times 10 \text{ cm}^3/\text{sec}$ . The thickness of this aquifer is revealed  $H=2.17\text{m}$ . The result of the drawdown test data analyzed by Jacob's method is shown in Fig.3.4. From this result a rough estimate of the permeability is obtained as  $K=1.12 \times 10^{-3} \text{ cm/sec}$ . For the relatively large time ( $t=20$  hours) drawdown test data of the observation well ( $r=15.7\text{m}$ ), the drawdown which is regarded as steady state is  $\zeta=17.5\text{cm}$ . Interpolating these values into Eq.(3.50), the rough calculation of the value of  $R$  is gotten

$$\begin{aligned} R &= r \cdot \exp(2\pi KH\zeta/Q) \\ &= 1.57 \times 10^3 \exp(2 \times 3.14 \times 1.12 \times 10^{-3} \times 2.17 \times 10^2 \times 17.5 / 2.67 \times 10^3) \\ &= 42.4\text{m} \end{aligned}$$

Though the Kamo river that is regarded as the constant head boundary exists at the distance  $R=1000\text{m}$  from the pumped well, for the reason that the pumping rate is small and the ground water supply is large because the region is the center of the Kyoto Basin, the value of the influence is estimated for cases, that is,  $R=25\text{m}$ ,  $30\text{m}$ ,  $40\text{m}$ , and  $50\text{m}$ . All observation wells have penetrations of  $z=2\text{m}$  and radial distance of each well is shown in Fig.3.3. Then, interpolating these values ( $z, R, r_1, \zeta, H$ ) into Eq.(3.49), the theoretical curves are gotten.

Matching the field results to the theoretical curves for each value of  $R$ , the field data make a satisfactory fit to the theoretical curves for  $R=30\text{m}$ , as shown in Fig.3.5. At the match point where  $\zeta^*=5.9 \times 10^{-1}$ , and  $t^*=2 \times 10^4$ , one reads  $\zeta=16\text{cm}$  and  $t=2.55 \times 10^4 \text{ sec}$  for  $r=15.7\text{m}$ . From Eq.(3.53) the permeability can be calculated

$$K = \frac{26.66 \times 5.9 \times 10^{-1}}{2 \times \pi \times 217 \times 16} = 7.21 \times 10^{-4} \text{ (cm/sec)}$$

From Eq.(3.54), the effective porosity can be calculated

$$s_y = \frac{7.2 \times 10^{-4} \times 2.55 \times 10^4}{2 \times 10^4} = 9.19 \times 10^{-4}$$

Interpolating these calculated values in Eq.(3.47), the result of comparison of theoretical curves with drawdown test data is shown in Fig.3.6. It is definite that theoretical curves give good match with the drawdown test data.

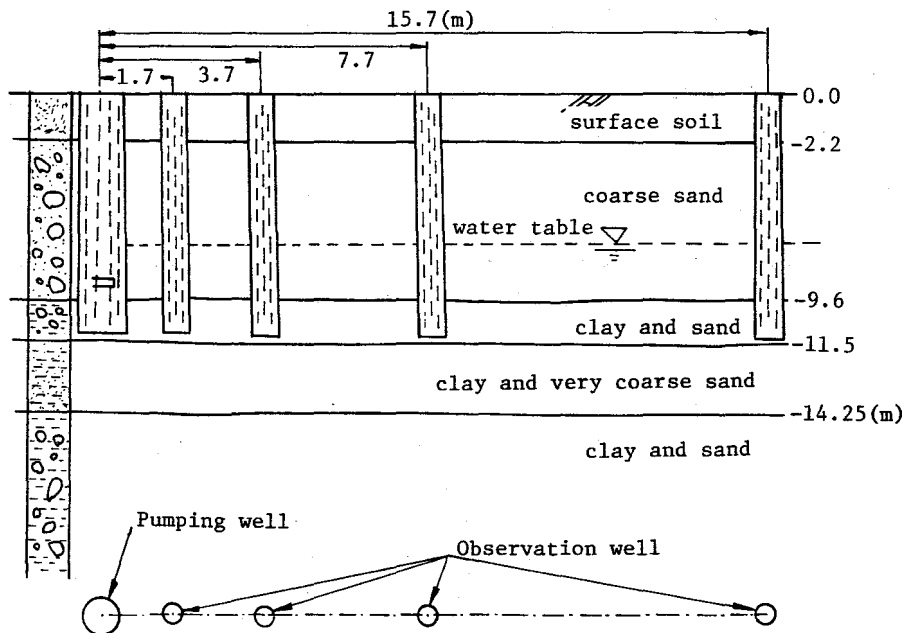


Fig.3.3 Hydrogeological cross-section of the drawdown test site

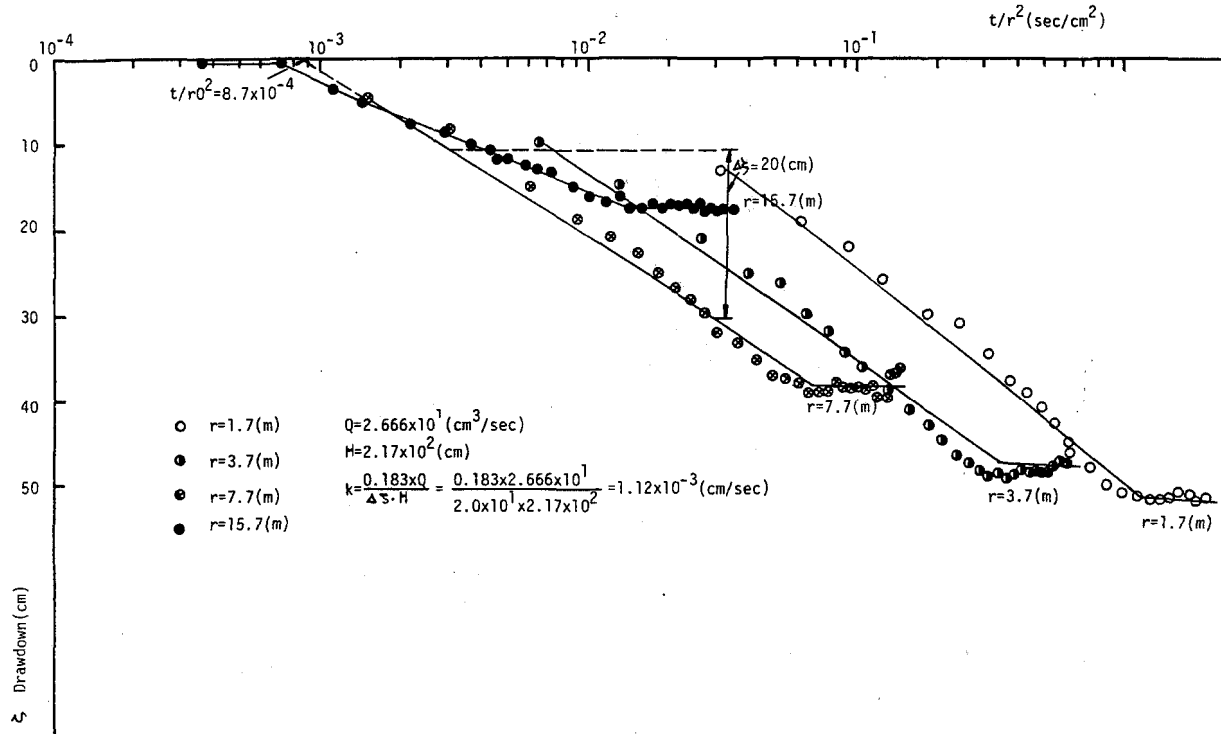


Fig.3.4 Method of Jacob's analysis ( $\zeta - t/r^2$ )

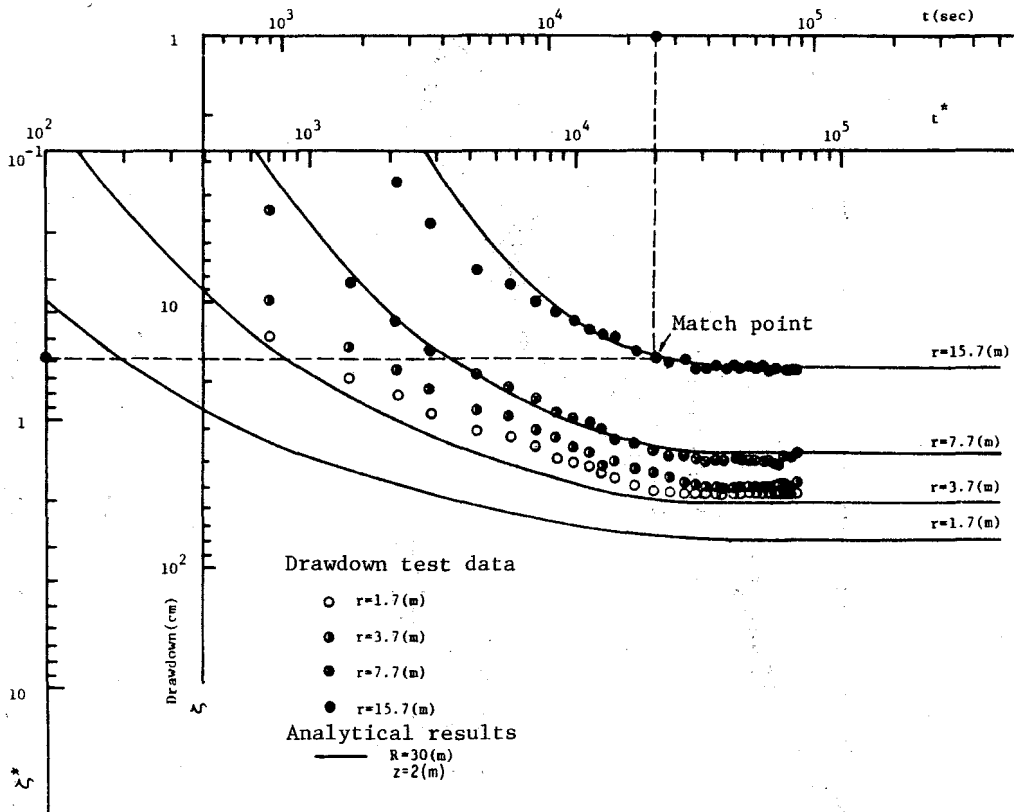


Fig.3.5 Method of superposition for finite region solution

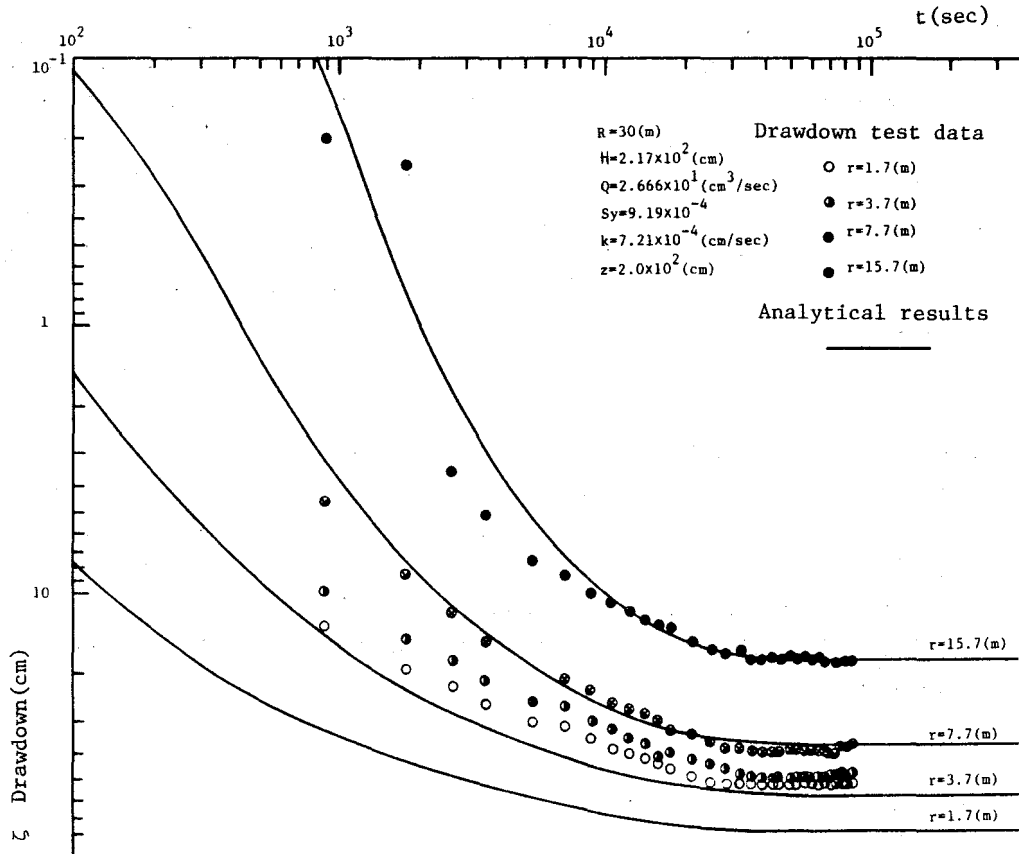


Fig.3.6 Comparison of the analytical results and drawdown test data

#### 4. Conclusions

In this paper formulas and methods available to evaluate the data from drawdown tests under a special condition have been developed. Namely, to analyze drawdown test data obtained in the much ground-water supplied region, a conception of "Island Model" has been applied in unsteady state. The results of this study can be used to analyze drawdown tests in order to measure the two aquifer parameters  $K$  and  $S$ . These analytical solutions are very complex, but they can be recognized that they have greater generality than previous solution.

The conclusions obtained in this paper are as follows;

- (1) The unsteady analytical solutions of phreatic flow due to drawdown test are derived in the conception of "Island Model" that the shape of groundwater level is fixed by the circular water supply both for confined and unconfined aquifer.
- (2) By using these solutions, the methods of analyzing drawdown test data performed in confined and unconfined aquifer are given.
- (3) The effect of influence region is evaluated, and a theoretical explanation of the assumption based on experiences was given.
- (4) The example analysis to determine permeability and storage coefficient are shown.
- (5) The propriety of the solutions is verified comparing the analytical results with the drawdown test data taken from a real aquifer project.

#### References

- [1] Mononobe, T.: Hydraulics, Iwanami Syoten, 1950, pp.472. (in Japanese)
- [2] Dagan, G.: The solution of the linearized equations of free-surface flow in porous media, Journal de Mecanique. Vol.5, No.2, 1966, pp.217-215.
- [3] Dagan, G.: Second order linearized theory of free surface flow in porous media, La Houille Blanche, Grenoble, France, 8, 1964, pp.901-910.